JOURNAL OF MATERIALS SCIENCE 10 (1975) 1351–1359

# Grain-boundary structure in an austenitic stainless steel

P. R. HOWELL, A. R. JONES, B. RALPH
*Department of Metallurgy and Materials Science, University of Cambridge, UK*

This paper considers to what extent the grain-boundary structure in a commercial material may be understood in terms of modern structural theories of crystal boundaries. It is shown that in one particular state (partially recrystallized) 78% of the boundaries, examined by transmission electron microscopy, could be said to contain the type of structure predicted by the theoretical approach (i.e. intrinsic dislocation arrays).

This paper goes on to examine not only the "equilibrium" component of the boundary structure (intrinsic dislocation arrays) but also looks at the perturbations created in this component by the presence of other, "non-equilibrium" components (such as topographical discontinuities, precipitates and extrinsic dislocations produced by the dissociation of "run-in" matrix dislocations).

## 1. Introduction

### 1.1. General

This paper considers the structure of grain boundaries observed in a commercial alloy based on a 20% Cr–25% Ni austenitic steel which contains approximately 0.50% Nb and 0.05% (C + N). In all cases, the thermomechanical history of the specimen material was such that the only precipitate formed had the niobium carbide structure [1]. The two major classes of heat-treatment used were: (1) cold worked and aged (for details see [2]); (2) cold worked, aged and recrystallized (for details see [3]).* For clarity, the thermo-mechanical state is referred to as either aged or recrystallized in the figure captions.

### 1.2. Theoretical models of grain-boundary structure and their application to a commercial alloy

In attempting to define the structure of grain boundaries, two interrelated approaches have been taken. These are: (1) coincidence-ledge and computational models which predict boundary structures in terms of regularly repeating structure units [4-6]; (2) secondary dislocation models where the dislocations are characterized with respect to a coincidence site, or median, structure [7-10].

In this paper, the latter model will be adopted since much evidence for this type of sub-structure has been obtained from electron microscopic investigations [11, 12] and from field-ion microscopic studies [13, 14]. However, it should be appreciated that both models are equivalent and that the secondary dislocation model used here can also be generated from the coincidence-ledge approach [15].

Detailed observation of a large number of boundaries suggests that the complete description of grain-boundary structures in a commercial multiphase system requires the characterization of four types of boundary defect. These are:

(1) intrinsic grain boundary dislocations, which may be defined as those secondary dislocations which are predicted by the various models and are a requirement of the boundary geometry;

(2) extrinsic grain-boundary dislocations, which may be defined as those boundary dislocations formed due to the dissociation of "run-in" matrix dislocations;

(3) topographical defects in the boundary plane (e.g. grain-boundary steps and the discontinuities existing between plane facets) which may be formed during the thermo-mechanical processing of the alloy;

(4) grain-boundary precipitates which form during the ageing treatments. The first three

*General examples of both aged and recrystallized alloys are given in Fig. 1a and b.

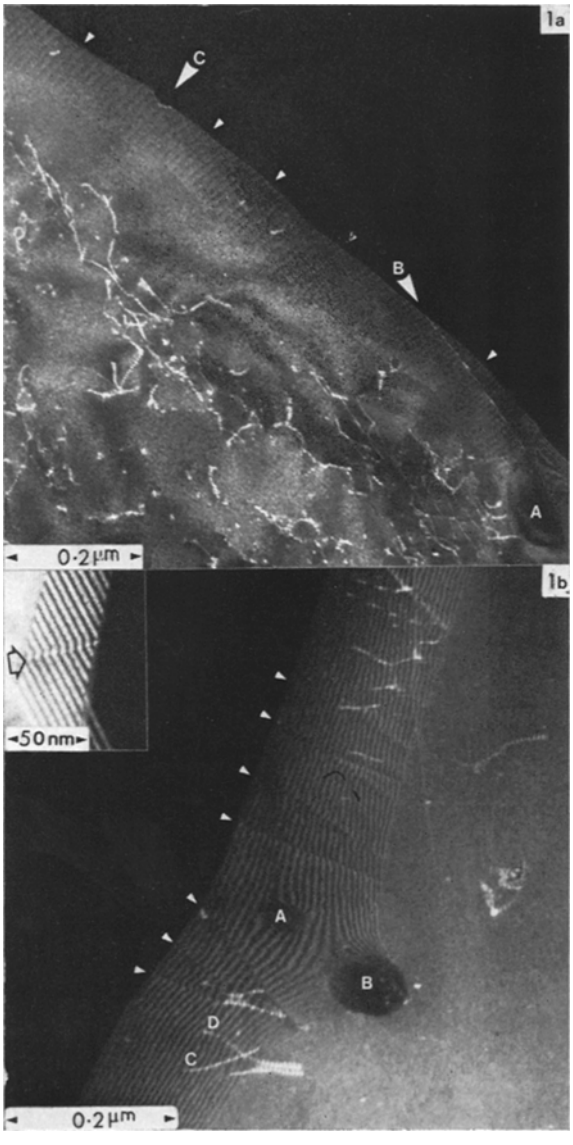


*Figure 1* General examples of the type of grain-boundary structures observed during the course of this investigation. (a) A weak beam micrograph of intrinsic grain-boundary dislocations in an aged alloy. A variety of other boundary defect types are observed in this micrograph (see text). (b) A weak beam micrograph of a variety of grain-boundary defect types in a recrystallized alloy. Interractions between matrix dislocations and the boundary are also observed at C and D.

classes of defect represent localized regions of relatively high strain energy, whilst the fourth class of defect is likely to interract with one or more of the first three classes leading to a modification of their structure and strain energy [2].

These major defect types may be illustrated with reference to Fig. 1a and b which show aged and recrystallized specimen material respectively. In Fig. 1a (which is a weak beam micrograph*), an array of intrinsic dislocations is observed (arrowed). A large precipitate (A) is seen to be associated with a change in boundary plane (B) and the presence of the precipitate (C) is seen to distort the local distribution of the intrinsic dislocations. A dislocation/precipitate depleted zone of the form described in [2], is observed in the vicinity of this boundary. In Fig. 1b a variety of "non-equilibrium" defects are observed in the absence of any resolved intrinsic dislocation array. Extrinsic dislocations are observed (arrowed), and considerable distortion of the boundary is observed in the vicinity of the precipitates (at A and B). A small step ($\simeq$ 2 nm in height) is shown on the inset to Fig. 1b.

### 1.3. Experimental techniques

Transmission electron microscopy of thin foils was used in this study since it allowed the fine scale defect structure of grain boundaries to be analysed using both normal imaging and diffraction modes. Weak beam microscopy has been used along with conventional bright- and dark-field imaging techniques. Similarly, conventional diffraction analysis has been used in conjunction with the analysis of grain-boundary diffraction events to determine the boundary parameters [17].

However, in certain cases, it was found that the determination of an axis/angle pair from straightforward diffraction analysis, was rendered difficult when the grain size of the material was small compared with the effective diameter of the standard diffraction apertures. This was found to be the case when partially recrystallized material was under investigation and a selected-area diffraction pattern taken over the central area shown in Fig. 2 included information from at least six grains. Hence, in order to examine the intrinsic dislocation structure of such boundaries, a series of centred dark field micrographs were taken, and each boundary in the area was imaged in at least three different diffracting conditions, such that each single boundary could be analysed in terms of the observed (or non-observed) intrinsic dislocation arrays. In this

*The application of weak beam microscopy to the analysis of grain-boundary structures is considered in more detail elsewhere [16].

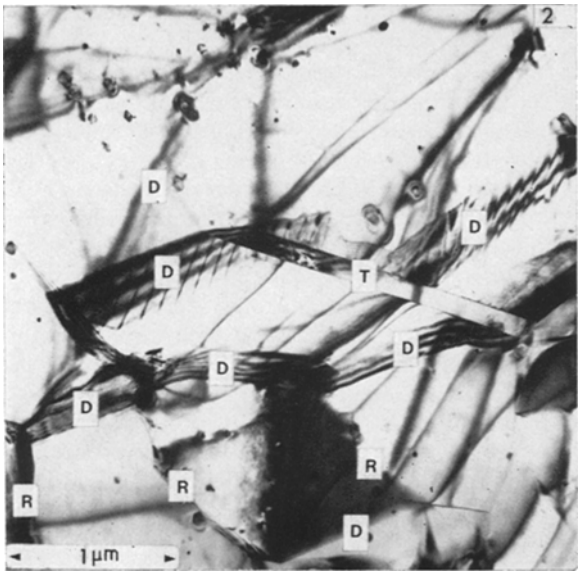


*Figure 2* A low magnification image (bright-field) of a recrystallized specimen. Those boundaries marked D exhibited intrinsic structure, those marked T were found to be fully coherent, whilst for those marked R no intrinsic structure was resolved.

manner, boundaries could be classed as: (1) exhibiting structure which could be characterized in terms of the modern dislocation models; (2) either incompatible with modern theory, or comprised of dislocation arrays whose spacing was below the working resolution limit of the technique.

Thus, by characterizing boundaries in terms of the observation of periodic intrinsic arrays of dislocations, in conjunction with standard diffraction analysis, a lower limit to the percentage of boundaries which conform to a dislocation type model of grain boundary structure could be found.

## 2. General

During the course of this investigation, over 500 grain boundaries were imaged and subjected to detailed analysis. The number of boundaries observed which contained intrinsic dislocation arrays varied as the thermo-mechanical history of the specimens varied, but the general applicability of a dislocation type model may be illustrated with respect to the partially recrystallized material shown in Fig. 2. In this particular micrograph, each boundary has been labelled either D, T or R where D = observation of boundaries containing intrinsic dislocations under two or more of three different diffracting conditions; $T$ = observation of fully coherent boundaries (e.g. primary twins); $R$ = observation of boundaries where no intrinsic dislocation arrays were found. As can be seen, the proportion of boundaries which contain structure which conforms to that predicted by a dislocation model of grain-boundary structure is very high, and the percentage number observed in this specimen material was found to be 78%.

This result is somewhat at variance with the predictions of Brandon [18] and Warrington [19]. However, it should be appreciated that the predictions of these authors relate to "simulated random polycrystalline aggregates", a situation unlikely to be realized in practice.

In all cases where the material under investigation had not been recrystallized, extrinsic dislocations were observed, and all boundaries, irrespective of specimen history, contained a variety of topographical defects, although the frequency of occurrence of each defect type was found to be a sensitive function of specimen history. Similarly, all boundaries were seen to be decorated with precipitates. Three major boundary/precipitate interractions were observed being: (1) interraction due to the nucleation and growth of precipitates at pre-existing defect structures in the boundary [2]; (2) interraction due to precipitate pinning of migrating grain boundaries [3]; (3) local migration of boundaries around coarsening boundary particles [20].

The above general observations indicate the complexity of boundaries observed in this

material, and the remainder of this paper will discuss in more detail the observation of the defect structures listed in Section 1.2. Section 3 discusses the observation of intrinsic dislocation arrays (i.e. the "equilibrium" boundary structure) while Section 4 discusses the observation of extrinsic dislocations, topographical discontinuities and grain-boundary precipitates (i.e. the "non-equilibrium" components of the structure).

## 3. Intrinsic grain-boundary dislocations

In general, observations pertaining to low-angle grain-boundary dislocations*, coincidence-site structure dislocations, and Van-der-Merwe dislocations showed them to be compatible with the various dislocation models, although these arrays were invariably modified by the presence of a variety of other boundary defects (see Section 1.2).

Fig. 3a to d show examples of intrinsic arrays as observed during the course of this study. The boundary dislocations observed in Fig. 3a are low-angle grain-boundary dislocations. The calculated axis/angle pair ([001]/3°) for this boundary is compatible with the measured defect spacing (4 nm), the deduced Burgers vector ($a/2$ [110]) and the line vector ([1$\bar{1}$0]). The above results concerning the defect spacing and character were confirmed by the observation of "fine structure" in the diffraction pattern (see Section 3 of [17]).

The boundary dislocations observed in Fig. 3b and c are coincidence-site structure dislocations characteristic of a $\Sigma = 5$ grain boundary. In Fig. 3b, one set of dislocations (A) is in contrast whilst in Fig. 3c (which is of the same boundary as that shown in (b) but using a different operating reflection) two sets of dislocations are observed (A and B). Those dislocations which are seen in enhanced contrast in Fig. 3b (A) are barely visible in Fig. 3c and the major source of diffracted intensity for this array is localized at the extrinsic dislocations (arrowed). The spacing of the two sets of dislocations shown in Fig. 3b and c, is 10 ± 1 nm (A) and 20 ± 1 nm (B) which yields a value, for the deviation from perfect coincidence of 0.3° (assuming that the Burgers vectors of the intrinsic dislocations are those predicted by the DSC lattice [7]†.

Fig. 3d shows an example of an array of grain-boundary Van-der-Merwe dislocations [10]. As may be seen, the spacing of the dislocations is non-uniform, which is due, in part, to the observed boundary curvature. This variation in spacing also occurs at discrete discontinuities in the boundary plane (e.g. at C and D) and these discontinuous changes in spacing indicate sharp changes in boundary inclination at these points.

The examples cited in this section show how grain boundaries may be seen to contain a variety of intrinsic dislocation arrays. However, these arrays are found to be complex due to interraction with a variety of other defect types which are not predicted by the various theoretical models. The observation of these "non-equilibrium" defects will be discussed in the next section.

## 4. "Non-equilibrium" boundary structure

### 4.1. Extrinsic grain-boundary dislocations

Extrinsic dislocations are the decomposition products of matrix dislocations which have been absorbed by a grain boundary during thermomechanical processing. The decomposition products are such that their Burgers vectors are compatible with the DSC vectors which characterize the intrinsic boundary dislocations [7].

During this study, the extrinsic dislocations were found to be stable in the boundary during examination even though one might expect some form of anihilation by rearrangement of the intrinsic dislocation array; this stability is presumably due to the pinning action of solute and/or precipitates. This point may be illustrated by referring to Fig. 4a which shows that the majority of extrinsic dislocations are decorated with precipitates. In this manner, the extrinsic dislocations are pinned, and dislocation rearrangement in the boundary plane is inhibited. Further examples of extrinsic dislocations are given in Figs. 1b and 4b; two sets of extrinsic dislocations with dissimilar lines being observed in both figures (arrowed). In certain cases, two sets with similar line vectors, but different Burgers vectors, were observed, and this aspect will be discussed in further reports.

In all cases, where extrinsic and intrinsic dislocations are observed (e.g. in Fig. 3b), the

*A low-angle grain boundary may be considered as a deviation from a $\Sigma = 1$ grain boundary where $\Sigma$ is defined as the reciprocal of the density of coincidence sites shared between the two grains [21].
†The DSC lattice is generated from the "O" lattice theory and predicts grain-boundary dislocation Burgers vectors

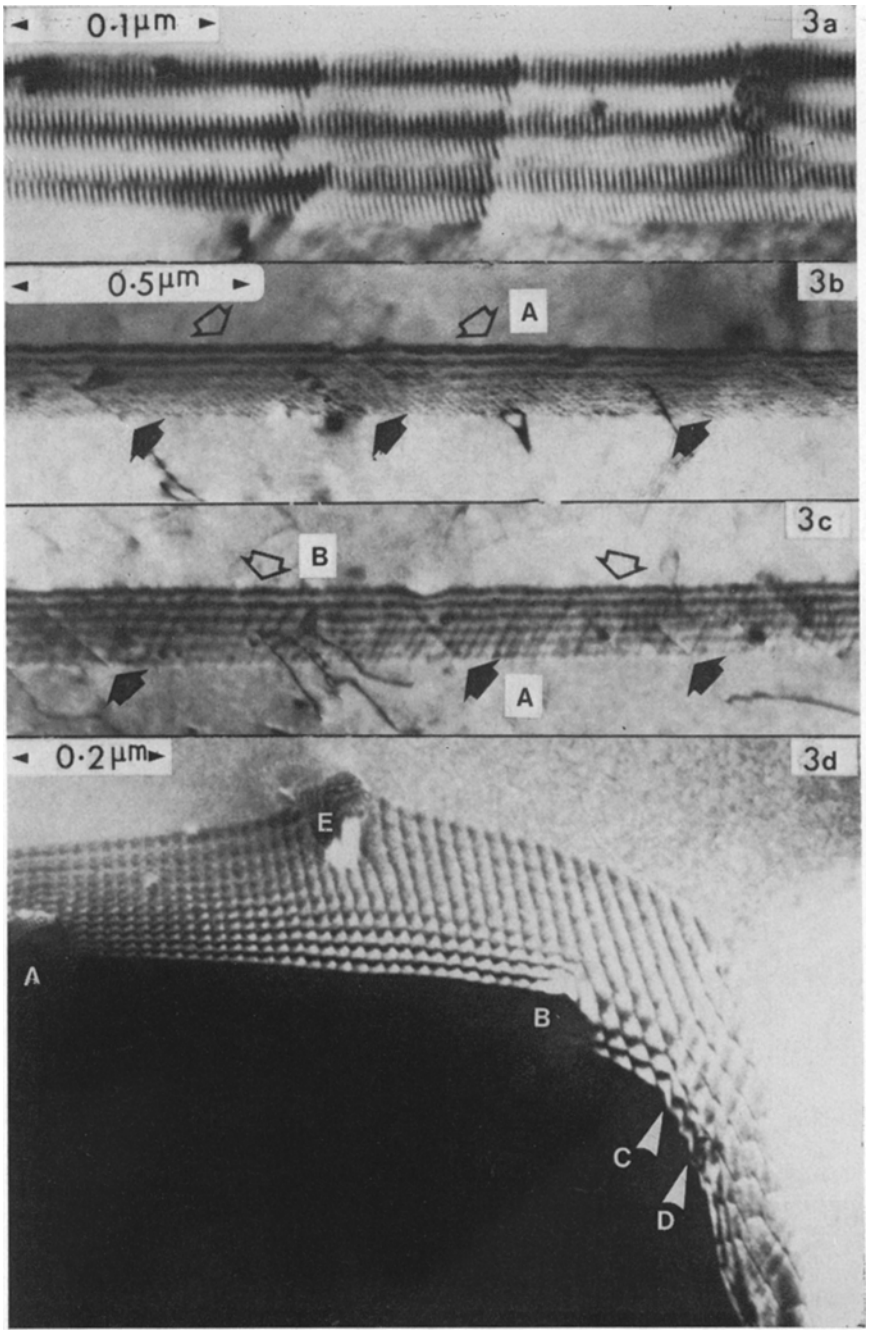


*Figure 3* Examples of intrinsic dislocation arrays observed in grain boundaries. (a) A low-angle grain boundary ([001]/3°). An array of edge dislocations is observed. This dislocation array gave rise to "extra reflections" in the diffraction pattern which confirmed the observations concerning the axis/angle pair determination and the dislocation analysis, see text (recrystallized). (b) Coincidence-site structure dislocations in a grain boundary which is close, in orientation, to a $\Sigma = 5$ configuration. One set of dislocations (A) is in contrast. The spacing of these dislocations is $10 \pm 1$ nm. The extrinsic dislocations (arrowed) are seen to be parallel to the intrinsic dislocations. (c) Same boundary as that shown in (b) but two sets of dislocations (A and B) are in contrast. However, those dislocations imaged in (b) (A) are only weakly diffracting and the contrast attributable to these dislocations is mainly localized to the parallel extrinsic dislocations (arrowed). The spacing of the second set of dislocations (B) is $20 \pm 1$ nm. Variations in the observed local spacing and orientation of both sets of intrinsic dislocations can be ascribed to micro-topographical defects in the boundary plane (aged). (d) An array of Van der Merwe dislocations in a high-angle grain boundary. The spacing and orientation of these dislocations changes as the orientation of the boundary plane changes which is due to curvature (A-B) and faceting (e.g. at C and D). Considerable distortion of the intrinsic dislocations is also seen in the vicinity of the boundary precipitate at E (recrystallized).

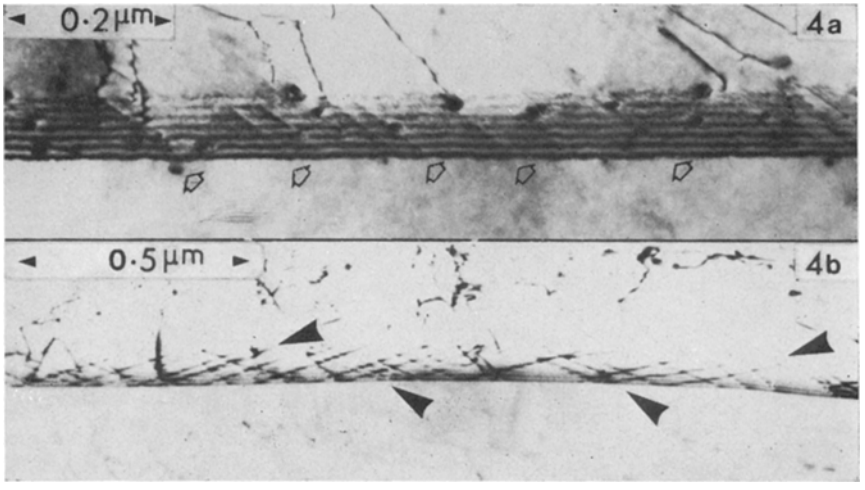


*Figure 4* Examples of grain-boundary extrinsic dislocations. (a) An array of parallel boundary extrinsic dislocations is observed (arrowed), and the majority of these dislocations are seen to be decorated with grain-boundary precipitates (aged). (b) Two sets of parallel extrinsic dislocations are observed (aged).

contrast in the vicinity of the extrinsic dislocations is enhanced with respect to those regions which contain only intrinsic dislocations. This observation implies that the strain field is increased in the vicinity of the extrinsic dislocations. This is not unexpected since the introduction of any dislocation defect into a periodic array must perturb the mutually reduced long-range strain fields of the component dislocations by locally changing the intrinsic dislocation spacing away from the equilibrium wavelength in that area. This local increase in strain field is important when a variety of thermo-mechanical properties are considered. Hence, Keg, *et al.* [22] found that extrinsic dislocations could move in the boundary giving rise to grain-boundary sliding. Similarly Jones *et al.* [2] found that these extrinsic dislocations were the dominant site for the nucleation and growth of boundary NbC precipitates.

### 4.2. Topographical defects

Topographical defects were observed in all grain boundaries examined during this study. These defects may be grouped into four main classes in terms of their effect on the overall geometry of the boundary being:

(1) steps in the boundary plane;

(2) discontinuous changes in the boundary plane (i.e. the junction between adjoining facets);

(3) triple junctions where three grains are in contact along a line;

(4) curvature in the boundary plane*.

Although it is difficult to predict the exact nature of these boundary defects, classes 1, 2 and 3 may be considered in terms of quasi-dislocation defects and/or localized residual displacement fields, whereas, for class 4, the continuously varying boundary orientation results in an intrinsic dislocation spacing which is non-uniform, and hence the phenomenon of mutually reduced long-range strain fields will be less apparent.

Figs. 3b and c and 5a show how steps in the boundary plane affect the intrinsic dislocation arrays. In Fig. 3b and c, the steps are identified by the variations in local dislocation spacing, and by the discontinuities observed in the depth fringes. The steps seen in Fig. 5a are more immediately apparent due to their larger height, and the steps (arrowed) are seen in enhanced contrast. In certain cases, periodic arrays of steps were seen where the "step height" was of the order of 3 nm or less, and an example of a single step of similar dimensions is given in Fig. 1b.

An example of the effect of faceting on the

*This list of topographical defects does not include the periodic ledge structure of Bishop and Chalmers [4] which arises as an alternative description of the "quasi-equilibrium" boundary structure.

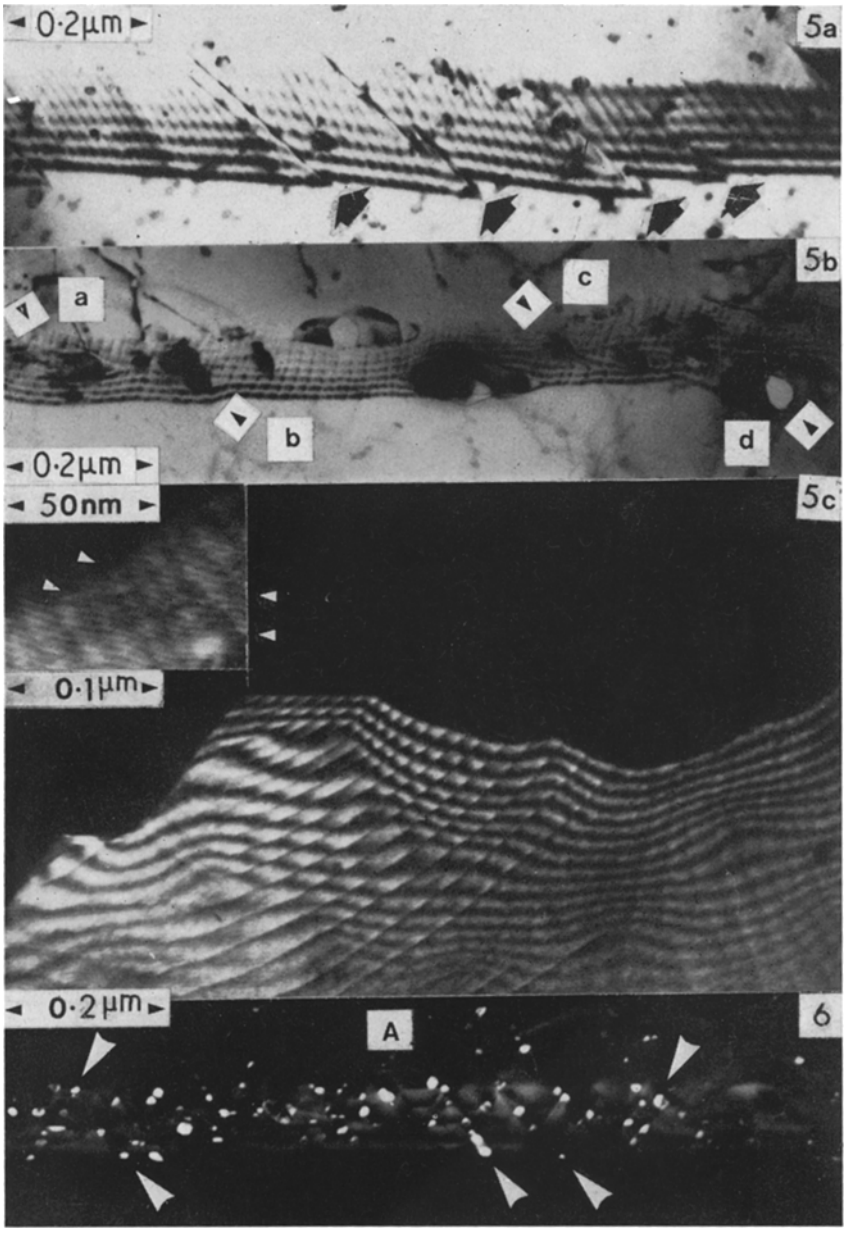


*Figure 5* Grain-boundary topographical defects. (a) A stepped low-angle grain boundary. The steps separate facets of similar, but not identical, orientation, namely, the slightly different intrinsic dislocation spacing on adjacent facets (recrystallized). (b) The effect of boundary curvature on the intrinsic dislocations; their lines are seen to be curved. Topographical defect precipitation is also observed here at a-b and c-d (aged). (c) The effect of boundary curvature on extrinsic dislocations. As with (b) their lines are seen to be curved. A set of very fine intrinsic defects is also observed in this boundary, see inset (recrystallized).
*Figure 6* A precipitate dark-field micrograph (using a precipitate 002 reflection characteristic of grain A) showing extrinsic dislocation precipitation, arrowed (aged).

character of intrinsic dislocation arrays was given in Fig. 3d, the spacing and orientation of the intrinsic dislocations being seen to change discontinuously.

Fig. 5b and c illustrate the effect of boundary curvature on observed dislocation arrays. In Fig. 5b, the curvature in the boundary is accompanied by intrinsic dislocations which have curved lines. This micrograph also illustrates enhanced precipitation on complex topographical discontinuities (arrowed). In Fig. 5c, the curvature in the boundary results in extrinsic dislocation lines being curved. This boundary exhibits a very complex character, and a set of very fine intrinsic defects ($\simeq$ 2.5 nm spacing) are observed in this boundary (arrowed on inset).

### 4.3. Grain-boundary precipitation

Precipitates on the grain boundary are bound to have a marked effect on boundary structure since they are:

(1) nucleated preferentially on extrinsic dislocations and topographical defects [2];

(2) pinning points for a migrating boundary [3];

(3) likely to introduce distortions into the intrinsic dislocation arrays.

Fig. 5b illustrates enhanced grain-boundary precipitation on complex topographical defects, whilst in Fig. 6, which is a precipitate dark-field micrograph, linear arrays of precipitates are seen to be associated with the two sets of extrinsic grain-boundary dislocations observed.

Although the identification of preferential precipitation on extrinsic dislocations is relatively unambiguous, the observation of precipitates on topographical defects may be due to the migration of the boundary around individual precipitates [20]. However, when a series of precipitates are seen to be associated with one particular topographical defect, it is likely that this defect was present prior to ageing and not formed during ageing.

The effect of precipitate pinning on a migrating boundary is shown in Fig. 1b, whilst distortions in intrinsic dislocation arrays due to the presence of grain-boundary precipitates are observed in Figs. 1a and 3d.

## 5. Conclusion

This paper has demonstrated how grain boundaries in a commercial alloy may be considered and analysed experimentally in terms of a variety of defect structures. The most important result concerns the very high proportion of boundaries which may be analysed in terms of modern structural theories since serious doubts about the range of applicability of these models has been voiced in the past. It has also been shown that a variety of other defects are present in grain boundaries, and these defects can often radically alter the character of the intrinsic dislocation arrays leading to the production of active sites for precipitation, sliding and a variety of other boundary dependent properties.

## Acknowledgements

The authors are grateful to Professor R. W. K. Honeycombe for the provision of laboratory facilities. Valuable discussions with Dr T. F. Page are acknowledged. Financial support from the Science Research Council and the Harwell and Springfield Laboratories of the United Kingdom Atomic Energy Authority is gratefully acknowledged.

## References

1. J. M. ADAMSON, D.Phil. Thesis, University of Oxford (1972).
2. A. R. JONES, P. R. HOWELL, T. F. PAGE and B. RALPH, In: "Grain Boundaries in Engineering Materials", Fourth Boulton Landing Conference (New York, 1974) in press.
3. A. R. JONES and B. RALPH, *Acta Met.* **23** (1975) 355.
4. G. H. BISHOP and B. CHALMERS, *Scripta Met.* **2** (1968) 133.
5. G. HASSON, M. BISCONDI, P. LAGARDE, J. LEVY and C. GOUX, In: "The Nature and Behaviour of Grain Boundaries", edited by Hsun Hu (Plenum Press, New York, 1972) p. 3.
6. H. GLEITER and B. CHALMERS, *Prog. Mat. Sci.* **16** (1972) 1.
7. W. BOLLMANN, "Crystal Defects and Crystalline Interfaces" (Springer-Verlag, Berlin, 1970).
8. M. J. MARCINKOWSKI and E. S. P. DASS, *Phil. Mag.* **26** (1972) 1281.
9. P. H. PUMPHREY, *Scripta Met.* **6** (1972) 107.
10. B. RALPH, P. R. HOWELL and T. F. PAGE, *Phys. Stat. Sol. (b)* **55** (1973) 641.
11. Y. ISHIDA, T. HASEGAWA and F. NAGATA, *J. Appl. Phys.* **20** (1969) 2182.
12. T. SCHOBER and R. W. BALLUFFI, *Phys. Stat. Sol (b)* **44** (1971) 275.
13. B. LOBERG, H. NORDEN and D. A. SMITH, *Arkiv. for. Fysik.* **40** (1970) 513.
14. P. R. HOWELL, Ph.D. Thesis, Univessity of Cambridge (1972).
15. P. R. HOWELL, A. R. JONES and B. RALPH, to be published.
16. *Idem*, to be published.
17. *Idem, J. Microsc.* **102** (1974) 323.
18. D. G. BRANDON, *Acta Met.* **14** (1966) 1479.
19. D. H. WARRINGTON, *J. Microsc.*, in press.

20. A. R. JONES, Ph.D. Thesis, University of Cambridge (1974).
21. D. G. BRANDON, B. RALPH, S. RANGANATHAN and M. WALD, *Acta Met.* **12** (1964) 813.
22. G. R. KEGG, C. A. P. HORTON and J. M. SILCOCK, *Phil. Mag.* **27** (1973) 1041.
Received 31 December 1974 and accepted 10 January 1975.